Supplementary information

Modulation of the Crystallization Dynamics via Multifunctional Additive Engineering to Achieve High-Performance Perovskite Solar Cells

Ling Han,[a,b] Hongbing Ran,[d] Yujun Liu,[b,c] Xinbo Ai,[b,c] Chao Zhou,[b] Fei Wang,[b] Xianfang Zhou,[b] Junsheng Wu,[b] Yonglei Han,[b,c] Qi Cao,[b,c] Yuxuan Feng,[b,c] Hai-lun Xia,[b] Kang Zhou,[b] Jingbai Li,[b] Hanlin Hu,[b*] Wang-Ting Lu,[a*], Shiyu Wang[b*] and Haoran Lin[b*]

[a]School of Optoelectronic Materials and Technology, Jianghan University, 8 Sanjiaohu Road, Wuhan, 430056, China.

[b]Hoffmann Institute of Advanced Materials, Shenzhen Polytechnic University, 7098 Liuxian Blvd., Nanshan District, Shenzhen, 518055, China.

[c]School of Materials and Metallurgy, University of Science and Technology Liaoning, 185 Qianshan Zhong Road, Anshan, 114051, China.

[d]Institute of Nano-Science and Technology, College of Physical Science and Technology, Central China Normal University, Wuhan, 430079, China.

[*]Corresponding author: Wang-Ting Lu, Shiyu Wang, Haoran Lin.

E-mail address: luwangting08@163.com (Wang-Ting Lu), 1978033405@qq.com (Shiyu Wang), hlin@szpu.edu.cn (Haoran Lin).

Experimental Section

Materials:

Methyl hydrazine-1-carbohydrazonothioate hydroiodide, $C_2H_9IN_4S$, CAS No.: 37839-01-3, Purity: 98%, Brand: McLin. [4-(7H-dibenzocarbazole-7-yl)butyl]phosphate,$C_{24}H_{22}NO_3P$, CAS No.: 2882156-63-8, Purity: 98%, Brand: Shenzhen RuiXun. PbI_2, CAS No.: 10101-63-0, Purity: >98%, Brand: TCI. $PbBr_2$, CAS No.: 10031-22-8, Purity: 99.999%, Brand: Libo Technology. CsI, CAS No.: 7789-17-5, Purity: 99.999%, Brand: Libo Technology. MABr, CH_6BrN, CAS No.: 6876-37-5, Purity: 99.5%, Brand: Great Cell Solar. MACl, CH_6ClN, CAS No.: 593-51-1, Purity: 99.5%, Brand: Great Cell Solar. FAI, CH_5IN_2, CAS No.: 879643-71-7, Purity: 99.5%, Brand: Great Cell Solar. Dimethylformamide. DMF, C_3H_7NO, CAS No.: 68-12-2, Purity: 99.8%, Brand: Sigma-Aldrich. Dimethyl sulfoxide. DMSO, C_2H_6OS, CAS No.: 67-68-5, Purity: >99.9%, Brand: Sigma-Aldrich. Chlorobenzene. CB, C_6H_5Cl, CAS No.: 108-90-7, Purity: 99.8%, Brand: Sigma-Aldrich. Isopropyl alcohol. IPA, C_3H_8O, CAS No.: 67-63-0, Purity: 99.8%, Brand: Sigma-Aldrich. Methanol. CH_3OH, CAS No.: 67-56-1, Purity: 99.8%, Brand: Sigma-Aldrich. C_{60}, CAS No.: 99685-96-8, Purity: 99.9%, Brand: Libo Technology. [6,6]-Phenyl-C_{61}-butyric acid methyl ester, PCBM, $C_{72}H_{14}O_2$, CAS No.: 160848-22-6, Purity: 99.9%, Brand: Libo Technology. Bathocuproine. BCP, $C_{26}H_{20}N_2$, CAS No.: 4733-39-5, Purity: 98%, Brand: McLin. Ag, CAS No.: 7440-22-4, Purity: 99.999%, Brand: Fuzhou Infusion Technology. ITO conductive glass substrate, Indium Tin Oxide glass, Specification: ≤15Ω/cm², Area: 0.04 cm², Brand: Libo Technology.

Device Fabrication:

Cleaning of ITO Substrate: The ITO conductive glass substrate was ultrasonically cleaned using detergent, deionized water, ethanol, and isopropyl alcohol subsequently, with each step for 15 minutes. After ultrasonic cleaning, the ITO glass substrate was treated using by UV-ozone surface cleaner for 15 minutes to complete the pretreatment of the conductive substrate.

Preparation of SAM Hole Transport Layer: The ITO conductive glass substrate was transferred into a nitrogen-filled glovebox. Then, a 0.5 mg/ml solution of 4PADCB in methanol (CH_3OH) was spin-coated on the ITO substrate at 4000 rpm for 40 seconds. After spin coating, the ITO/4PADCB film was annealed at 100°C for 10 minutes. To clean the ITO/4PADCB film, an IPA solution was spin-coated at 5000 rpm for 30 seconds, and then annealed at 100°C for 5 minutes. The final ITO/4PADCB film was obtained.

Preparation of Perovskite Layer: A 1.63 M solution of $Cs_{0.05}(MA_{0.08}FA_{0.92})_{0.95}Pb(I_{0.976}Br_{0.024})_3$ was dissolved in 1 mL of mixed solvent (V_{DMF}:V_{DMSO} = 4:1) with 9% excessive PbI_2. The perovskite precursor solution was spin-coated using a two-step process: first at 1000 rpm for 10 seconds, followed by 4000 rpm for 40 seconds. Additionally, 150 μL of chlorobenzene (CB) anti-solvent was dropped onto the film substrate 10 seconds before the end of the spin-coating process. Finally, the perovskite film was annealed at 100℃ for approximately 30 minutes. For the target device, 0.3 mg of methyl hydrazine-1-carbohydrazonothioate hydroiodide solid was added to 1 mL of the pre-prepared perovskite precursor solution and stirred with a magnetic stirrer for 1 hour before use. The following steps are the same. The final ITO/4PADCB/PVSK film was obtained.

Preparation of Electron Transport Layer: Next, 20 mg PCBM was dissolved in 1 ml CB solvent. The solution was spin-coated onto the film substrate at 1500 rpm for 45 seconds, resulting in an ITO/4PADCB/PVSK/PCBM film. Then, using a vacuum deposition system, C_{60} was further deposited to optimize the electron transport layer. The deposition was performed at a rate of 0.1 Å/s, with a total thickness of 10 nm. The final ITO/4PADCB/PVSK/C_{60}-PCBM film was obtained.

Preparation of Buffer Layer: Using a vacuum deposition system, BCP was deposited at a rate of 0.1 Å/s with a thickness of 10 nm, covering the surface of the film. The ITO/4PADCB/PVSK/C_{60}-PCBM/BCP film was obtained.

Preparation of Electrode: Using a vacuum deposition system, Ag was deposited at a rate of 0.2-1.0 Å/s, with a total thickness of 100 nm. The complete ITO/4PADCB/PVSK/C_{60}-PCBM/BCP/Ag device was obtained.

Characterizations:

X-ray photoelectron spectroscopy (XPS) was performed by Thermo Scientific K-Alpha. Ultraviolet photoelectron spectroscopy (UPS) measurement was performed on Thermo ESCALAB 250XI. The ^{1}H NMR spectra were measured with JNM-ECZS series FT 400 Hz. The J–V curves characteristics of the PSCs devices were assessed using an IVS-KV6000 Enlitech sunshine simulator fitted with an AM 1.5G filter at 100 mW cm^{-2} and a Keithley SMU source after adjusting the light intensity using a standard calibration cell. Powder X-ray diffraction (PXRD) was measured at an incident angle of 3°-40° by using Bruker D8-Advances (Cu Kα radiation).The scanning electron microscope (SEM) images were performed with JSM-IT800 to observe the morphology of the perovskite thin film. The atomic force microscopy (AFM) images were performed on the Brucker Icon. The Kelvin probe force microscopy (KPFM) images were obtained by Bruker Dimension Icon. Edinburgh FLSP1000 spectrophotometer with 440 nm picosecond pulsed diode laser excitation source was used to quantify static PL and TRPL of perovskite film. A QE-R equipment from Enli Technology Co. Ltd. was used to acquire the matching EQE spectrum in the air. Grazing-incidence wide-angle X-ray scattering (GIWAXS) measurements were performed with SAXS Focus 3.0 equipped with a Cu X-ray Source (8.05 keV, 1.54 Å) and an EIGER 2R 500K detector. TOF-SIMS experiments were performed using a TOF-SIMS IONTOF M6 instrument (IONTOF GmbH). Dark J-V curve and Mott−Schottky plot measurements were carried out using AMETEK ParSTAT MC electrochemical workstation.

Theoretical calculation:

The DFT calculations used ORCA 5.0.4 program and employed the cc-pVDZ-pp basis set and SK-MCDHF-RSC effective core potential for Pb and I atoms.

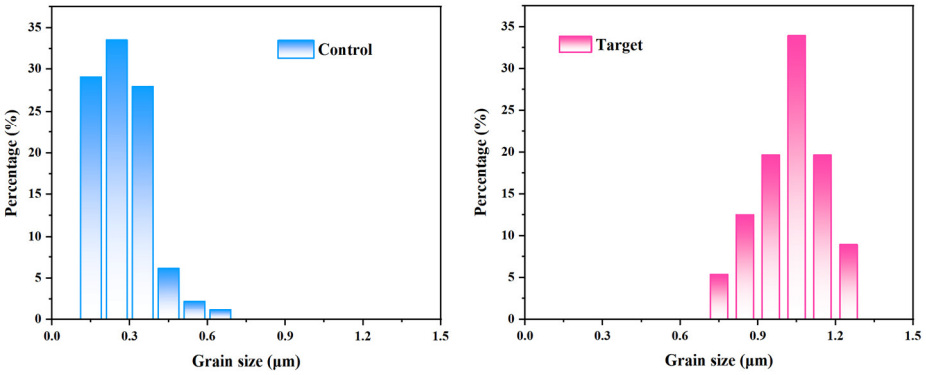

Fig. S1. Grain size distribution of the control and target films.

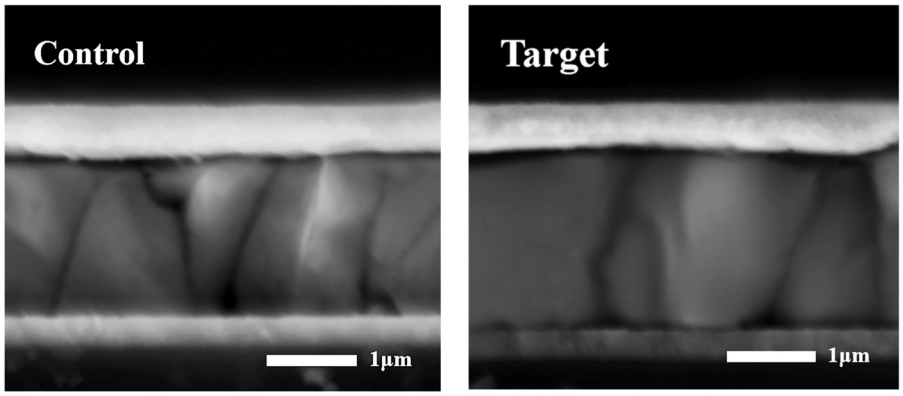

Fig. S2 Cross-sectional images of the control and target devices.

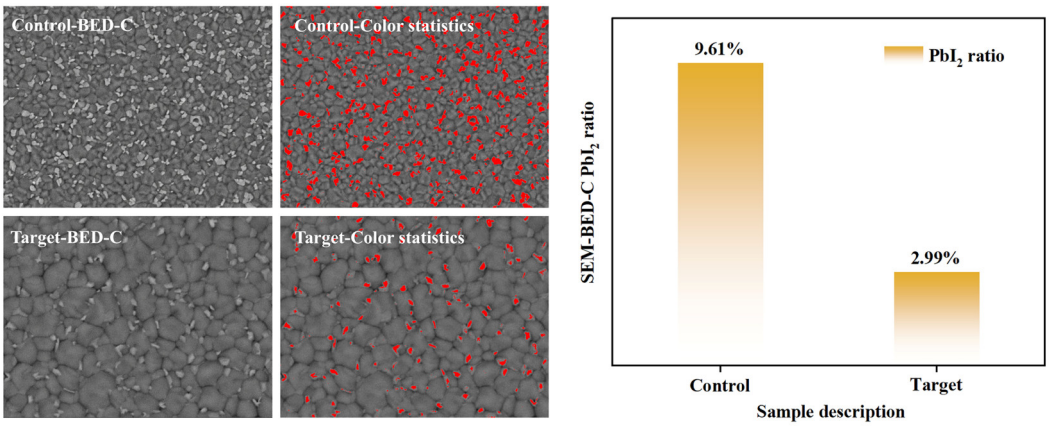

Fig. S3. The distribution and PbI_2/perovskite area ratios of PbI_2 regions on the control and target films.

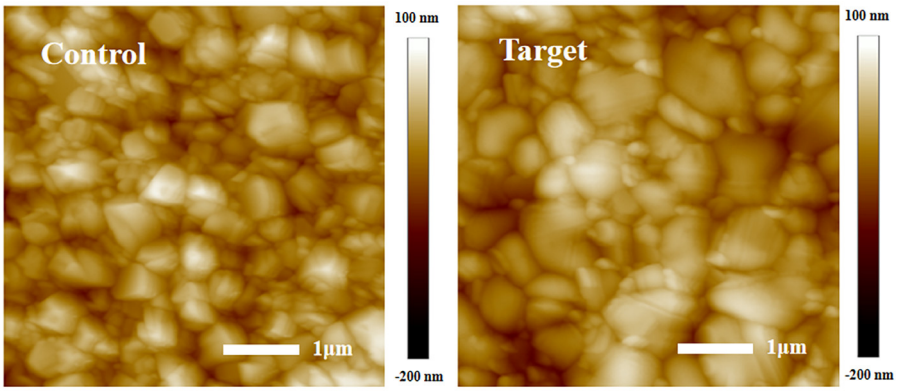

Fig. S4.Top-view AFM height images of the control and target films.

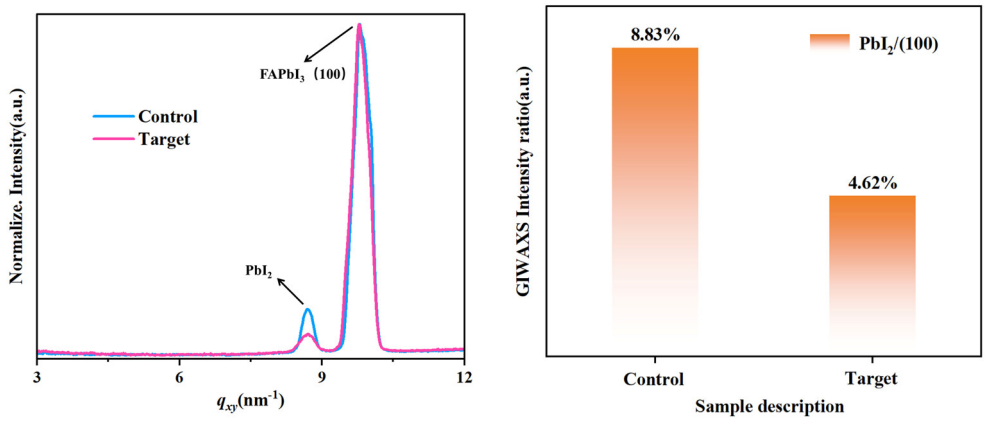

Fig. S5. 2D GIWAXS patterns of the control and target films at the q_z direction, with X-ray incident angle of 1° and the integrated intensity ratios of PbI_2/(100) peaks.

.

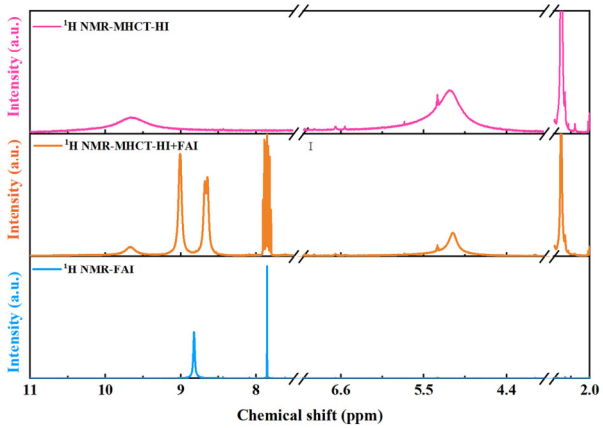

Fig. S6. ^{1}H NMR spectra of MHCT-HI, FAI and MHCT-HI+FAI in DMSO-d_6.

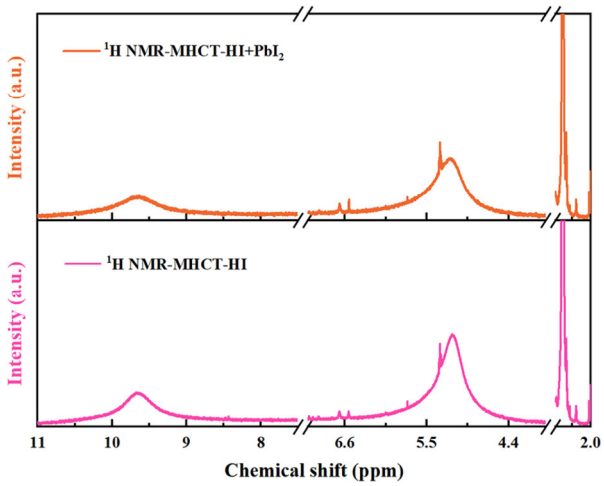

137

138 **Fig. S7. ^{1}H NMR spectra of MHCT-HI, and MHCT-HI+PbI$_2$ in DMSO-d$_6$.**

139

140

141

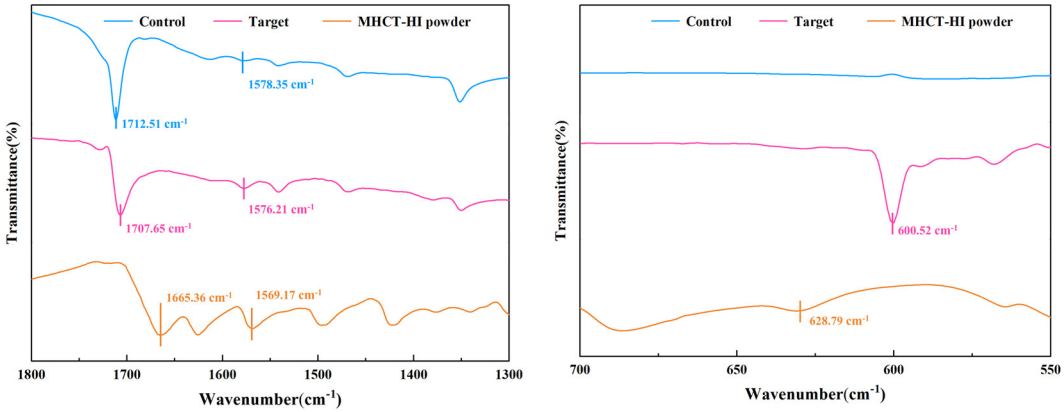

142

143 **Fig. S8. ATR-FTIR spectra of the MHCT-HI powder, control film, and target films.**

144

145

146

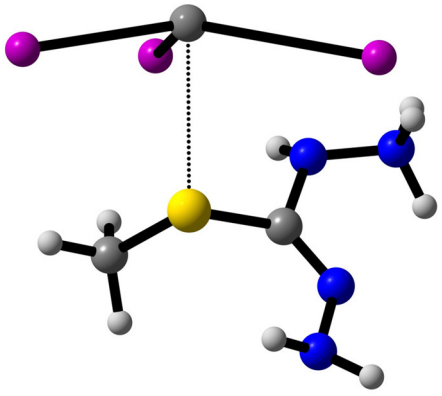

147

148 **Fig. S9. Density functional theory (DFT) calculation.**

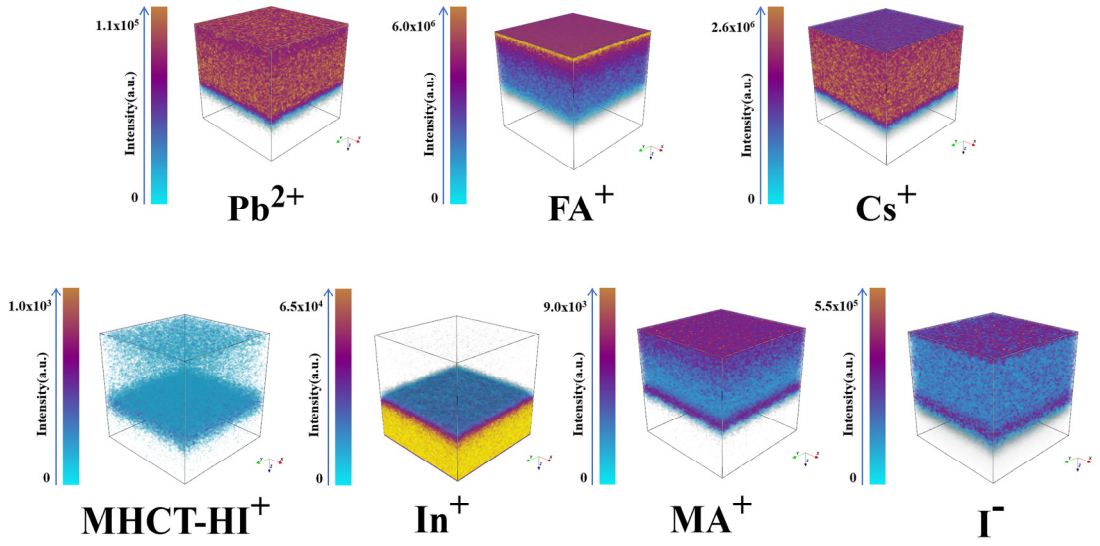

149

150 **Fig. S10.3D depth distribution of Pb^{2+}, FA^{+}, MA^{+}, MHCT-HI^{+}, Cs^{+}, I^{-}, and In^{2+} ions in the target**
151 **film.**

152

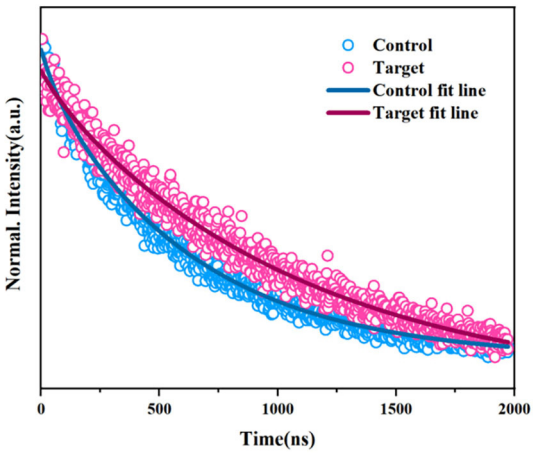

153

154 **Fig. S11. TRPL spectra of the control and target films.**

155

156

157

158

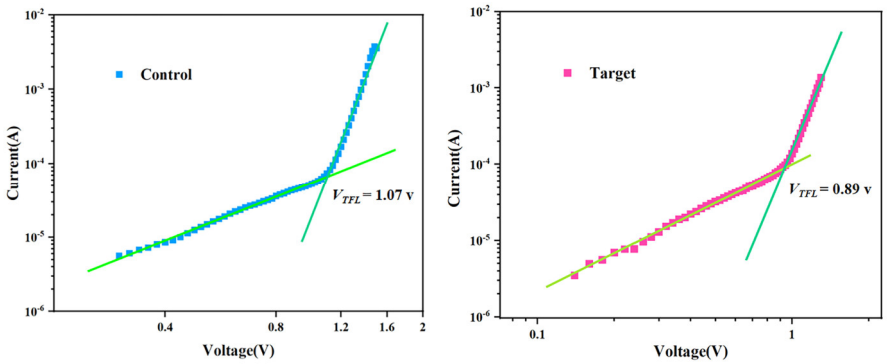

159

160 **Fig. S12. SCLC characteristics of the hole-only devices.**

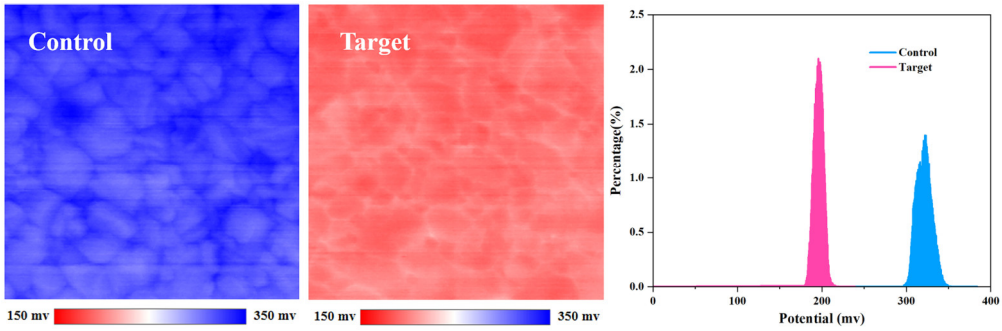

Fig. S13. CPD mapping and distributions of the control and target films.

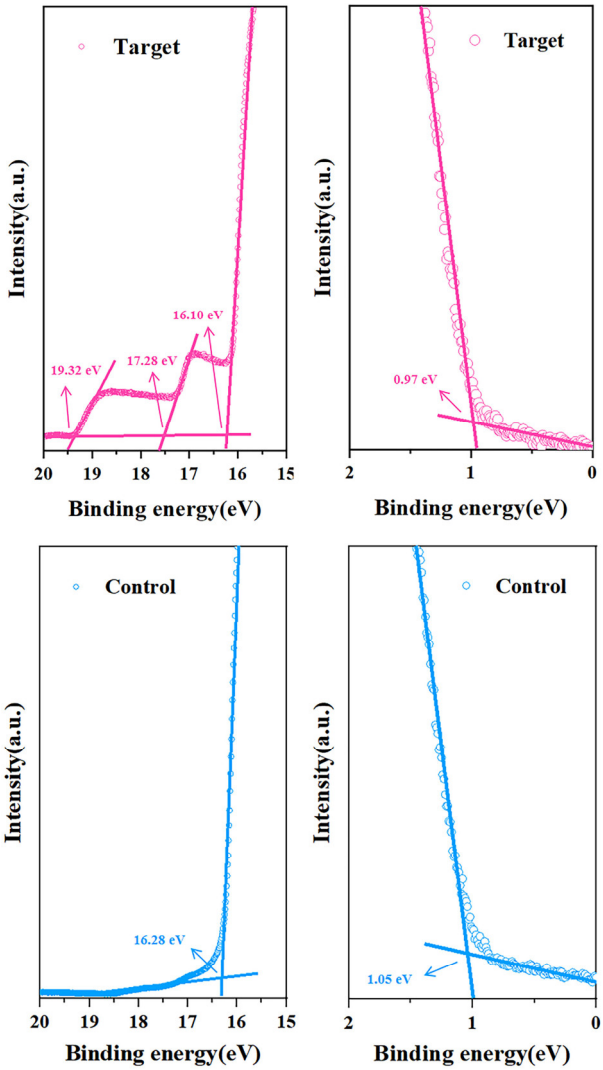

Fig. S14.The secondary electron cutoff and Fermi edges in the UPS spectra of the control and target films.

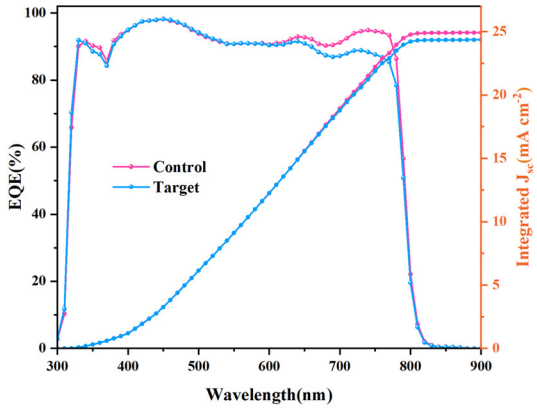

Fig. S15.EQE curves and the integrated J_{SC} of the control and target devices.

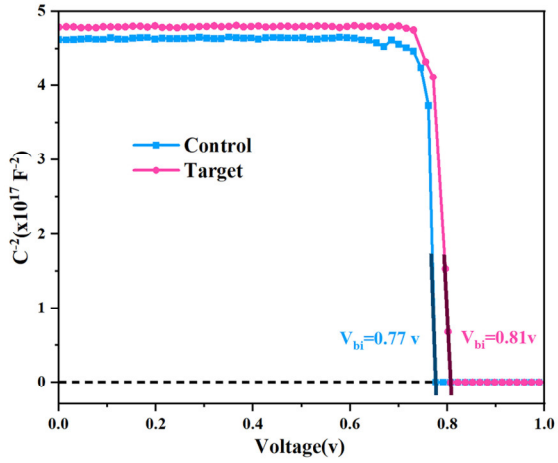

Fig. S16.Mott-Schottky curves of the control and target devices.

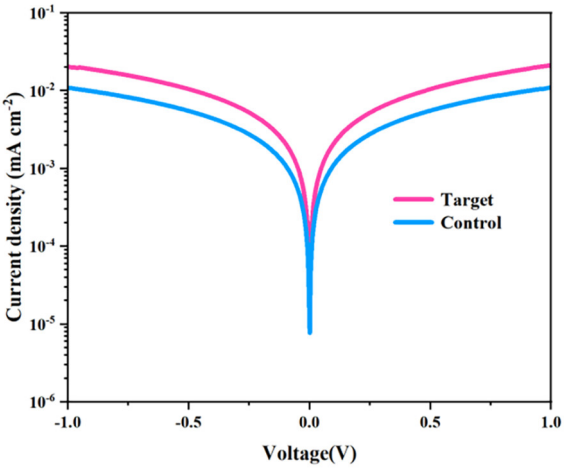

Fig. S17. Dark *J-V* curves of the control and target devices.

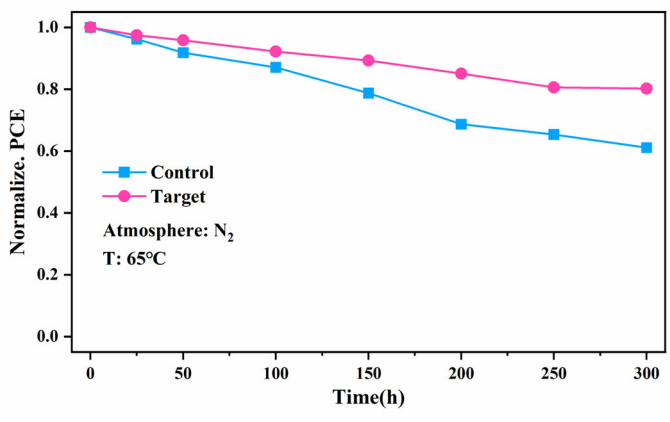

Fig. S18. PCE of the unencapsulated control and target devices under continuous 65°C heating in nitrogen.

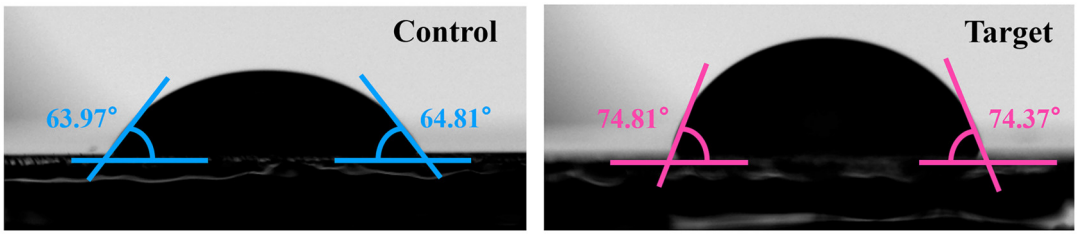

Fig. S19. Water contact angles of the control and target films.

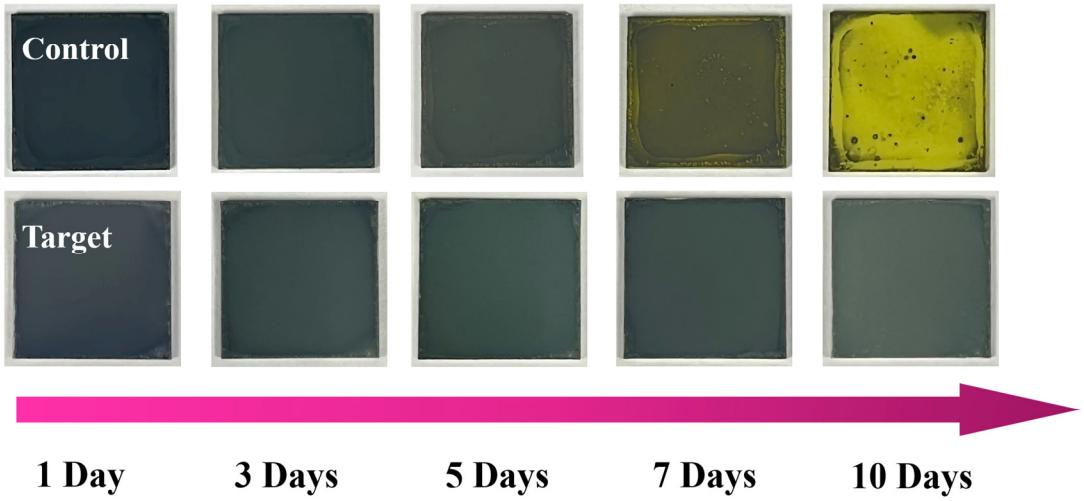

Fig. S20. The optical images of the control and target films in 10 days.

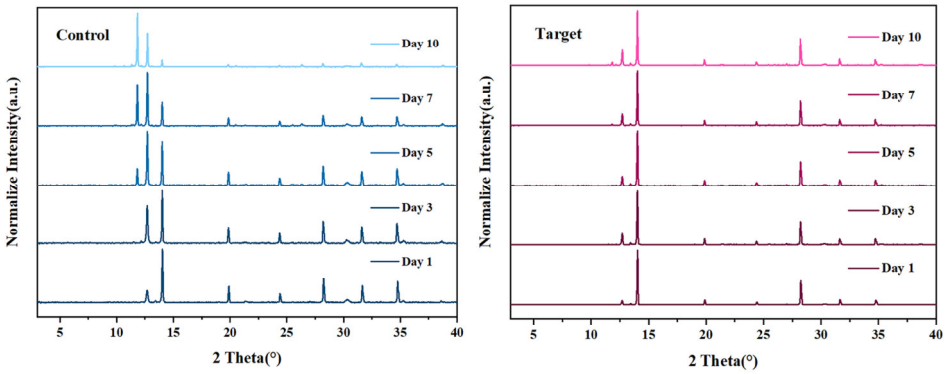

Fig. S21. The PXRD patterns of the control and target films in 10 days.

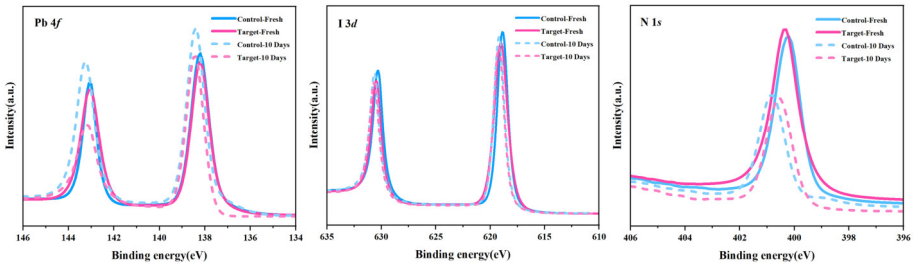

Fig. S22. The Pb *4f*, I *3d* and N *1s* XPS spectra of the fresh and aged control and target films.

Table S1.The fitted PL decay parameters of the control and target films

	τ_1(ns)	A_1(%)	τ_2(ns)	A_2(%)	τ_{avg}(ns)
Control	73.69	8.5	629.03	91.5	623.05
Target	108.453	4.5	1087.57	95.5	1082.99

The PL decay curves were fitted by a double exponential function:

$$y = y_0 + A_1 * e^{-\frac{x}{\tau_1}} + A_2 * e^{-\frac{x}{\tau_2}}$$

where τ_1 and τ_2 represent a fast and slow decay component.

The average lifetimes of perovskite films were calculated by the follow equation:

$$\tau_{ave} = \frac{A_1\tau_1^2 + A_2\tau_2^2}{A_1\tau_1 + A_2\tau_2}$$

Table S2. The performance of over 20 PSC devices with varied additive concentrations.

	$V_{OC,\ avg}$(V)	$J_{SC,\ avg}$ (mA cm^{-2})	FF $_{avg}$ (%)	PCE $_{avg}$ (%)
Control	1.128±0.01	25.14±0.24	78.96±1.19	22.38±0.30
w/0.1 mg/ml MHCT-HI	1.128±0.01	25.75±0.16	80.62±1.26	23.41±0.35
w/0.3 mg/ml MHCT-HI	1.145±0.01	25.78±0.22	83.28±0.27	24.55±0.26
w/0.5 mg/ml MHCT-HI	1.139±0.01	25.56±0.29	80.78±1.14	23.51±0.34